Vol 17 No 6, June 2008
1674-1056/2008/17(06)/2292-05

Chinese Physics B

© 2008 Chin. Phys. Soc.
and IOP Publishing Ltd

Electrical and deep levels characteristics of ZnO/ Si heterostructure by MOCVD deposition*

Liu Ci-Hui(刘磁辉)[a)†], Liu Bing-Ce(刘秉策)[b)], and Fu Zhu-Xi(付竹西)[a)]

[a)] *Department of Physics, University of Science and Technology of China, Hefei* 230026, *China*

[b)] *Department of Electron Science and Technology, University of Science and Technology of China, Hefei* 230026, *China*

(Received 8 June 2007; revised manuscript received 28 January 2008)

ZnO films have been prepared on p-type Si substrates by metal-organic chemical vapour deposition (MOCVD) at different total gas flow rates. The current versus voltage and temperature ($I-V-T$) characteristics, the deep-level transient spectroscopy (DLTS) and the photoluminescence (PL) spectra of the samples were measured. DLTS shows two deep-level centres of E_1 (E_C–0.13±0.02 eV) and E_2 (E_C–0.43±0.05 eV) in sample 1202a, which has a ZnO/p-Si heterostructure. A deep level at E_C–0.13±0.01 eV was also obtained from the $I-T$ characteristics. It was considered to be the same as E_1 obtained from DLTS measurement. The emission related to this deep level center was detected by PL spectra. In addition, the energy location and the relative trap density of E_1 was varied when the total gas flow rate was changed.

Keywords: MOCVD, ZnO/ Si heterostructure, PL spectra, deep-level emission
PACC: 8115H,7340L,7855,7155G

1. Introduction

Short-wavelength optoelectronic materials that can be used in ultraviolet (UV) lasers and light-emitting diodes have received much attention in the past decades. Researches on ZnO have been conducted more than 20 years, and many productions have already been in practical applications.[1−8] However, in recent years, ZnO films have attracted much attention due to their UV emission.

ZnO films can be grown by many different methods such as magnetron sputtering, spray pyrolysis, sol-gel technique, pulsed laser deposition, molecular beam epitaxy and metal-organic chemical vapour deposition (MOCVD). The method of MOCVD has been the most promising method for its advantages in growing high quality films and large-scale production compatibility.[9]

Deep levels in the forbidden band of ZnO play an important role in luminescence. Some of them can act as recombination centres, which will reduce the luminous efficiency. While, others can be radiation centres which are useful for the luminous.

In this paper, optical and electric properties of ZnO/P-Si heterostructures grown by MOCVD are investigated using $I-V-T$ characteristics, DLTS and PL spectra measurements. The deep levels in the ZnO films are detected and the behaviour of them is investigated as well.

2. Experiment

Si(100) wafers with the resistivity (ρ) of 1Ω.cm were used as the substrates. Undoped ZnO films were grown on these substrates in a vertical MOCVD reactor at low pressures. The MOCVD system has been described in our previous study.[10] Diethyl zinc (DEZ) and carbon dioxide (CO_2) gas were used as the precursors. High purity nitrogen (N_2) was used as the carrier gas for DEZ. The temperature of the DEZ bubbler was kept at 10°C during the growth, and the flow rate of the N_2-carried DEZ and CO_2 was kept at 10 and 50 sccm respectively. Besides the N_2 carrier gas for DEZ, another N_2 gas line called N_2 'eluting gas' was injected from the top of the reactor for the purpose of obtaining a high gas velocity on the surface of the substrate. The flow rate of the N_2eluting gas was varied from 0.86 to 1.7 slm. The pressure in the chamber during the growth was kept at 133 Pa, and the growth temperature was 600°C. In order to improve the quality of ZnO films, all the films were annealed in air ambient

*Project supported by the National Natural Science Foundation of China (Grant Nos 50472009, 10474091 and 50532070).
†Corresponding author. E-mail: chliu@ustc.edu.cn

(humidity: 23%) at 700°C for 1 h after growth.

A 0.001Hz ultralow frequency sawtooth wave generation (Model 439 Function generator) was used as the voltage source for $I-V-T$ measurement. During the measurement, the samples were kept in a dark chamber. More experimental details can be found in Ref.[11]. DLTS measurements were performed in a temperature range within 77–400 K using NJ.M.DLTS. For comparison, the DLTS characteristics of p-Si(100) substrates were investigated with Al/p-Si Schottky structure. No deep level centre was detected. PL spectra were measured with a Model 850 fluorescence spectrometer.

3. Results and discussion

3.1. $I-V$ characteristics

Figure 1 shows the current-voltage characteristics of sample 1202a. There is a forward transition voltage at about 1.5 V. When the applied voltage is higher than 1.5 V, the forward current has an exponential relationship with the applied voltage. The current shown in Fig.1 has the general form[12]

$$I_{\mathrm{F}} = I_0 \exp\left(qV_{\mathrm{F}}/nkT\right), \tag{1}$$

where $I_0 = A^* S T^2 \exp\left(-q\phi_{\mathrm{B}}/kT\right)$ is the saturated leakage current, V_{F} is the bias voltage, n is the ideal factor, k is the Boltzmann's constant, T is the absolute temperature, A^* is the effective Richardson constant, S is the effective junction area and ϕ_{B} is the barrier offset. The fitting result shows that $n \approx 16$ ($V_{\mathrm{F}} \leqq 1.5$ V) and $n \approx 35$ ($V_{\mathrm{F}} > 1.5$ V). The large series resistance of the non-ideal heterojunction is considered to be the main reason for such large values of n. Therefore, Eq.(1) should be modified as follows (Eq.(2)):

$$V_{\mathrm{F}} = \frac{kT}{q} \ln\left(\frac{I_{\mathrm{F}}}{A^* T^2}\right) + \phi_{\mathrm{B}} + I_{\mathrm{F}} R_{\mathrm{on}}. \tag{2}$$

The first two terms in Eq.(2) are the voltage drops of the ideal heterojunction, and $I_{\mathrm{F}} R_{\mathrm{on}}$ is the voltage drop of the series resistance. Due to the low electronic mobility of ZnO film, the voltage drop of the series resistance may increase sharply with the increase of the current, results in the deviation from ideal factor n. Moreover, the surface states at different bias voltages which affect the barrier height may be another reason to this deviation.[13,14]

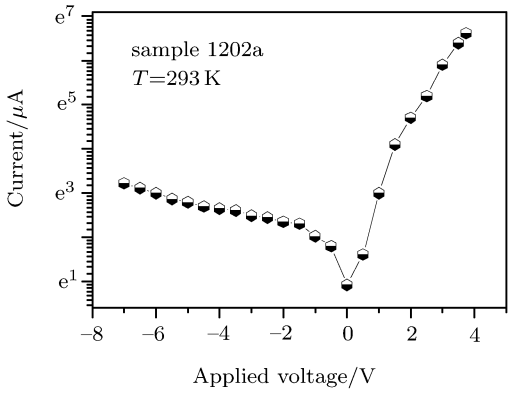


Fig.1. Current-voltage characteristic of ZnO/P-Si heterojunction.

3.2. DLTS measurements

The ZnO-ZnO grain boundaries can be modelled by double-Schottky-barrier junction.[15] When ZnO grains bond with Si layer, the crystal boundary between them can be regarded as intergranular boundary. In polycrystalline ZnO films, the donor density near the surface is lower than that in the bulk, while near the semiconductor/substrate interface, the donor density is even much lower.[16] From the capacitance-voltage measurement, the donor density in the layer near the surface of grains in sample 1202a is found to be in the range from 7.4×10^{14} to 2.3×10^{15} cm^{-3}, which is similar to that of pure ZnO crystal in Ref.[15]. There are many oxygen vacancies ($V_{\mathrm{O}}^{/}$) in ZnO grains. After annealing, the oxygen diffuses into the bulk. As a result, the donor density near the surface becomes lower. During the DLTS measurement, the space charge regions will extend to the ZnO grain near the surface layer.

Figure 2 shows DLTS spectroscopy of sample 1202a. Based on the DLTS theory,[17] the electron emission rate e_n can be expressed as

$$e_{\mathrm{n}} = (\sigma_{\mathrm{n}} \nu_{\mathrm{n}} N_{\mathrm{c}}) \exp(-E_{\mathrm{T}}/kT_{\mathrm{p}}), \tag{3}$$

where σ_{n}, v_{n}, N_{c}, E_{T}, T_{p} are the electron capture cross sections, the mean thermal velocity, the effective density of states in conduction band, the trap level emission peak temperature respectively. Two deep levels E_1 and E_2 (shown in Fig.2) are obtained. From the Arrhenius plots of $\ln(e_{\mathrm{n}}/T^2)$ versus $1/T$ (see Fig.3) and the intensity of the DLTS peaks (see Fig.2), the deep level positions and the relative trap density ($N_{\mathrm{t}}/N_{\mathrm{B}}$) can be found, where N_{t}

and N_B are the concentration of the defect and the doping concentration, respectively. It is found that $E_1 = E_C$–0.13±0.02 eV, N_t/N_B=1.01% and $E_2 = E_C$–0.43±0.05 eV, N_t/N_B=5.10% (E_C is the bottom of conduction band). The more parameters obtained are shown in Table 1. As we can see, the deep levels are affected by the flow rate of eluting gas. The locations and the relative trap density of deep levels for different samples are listed in Table 1.

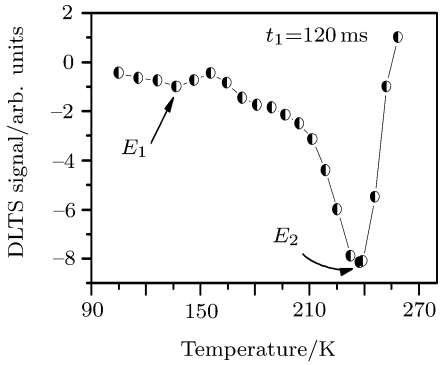


Fig.2. DLTS temperature scan of sample 1202a.

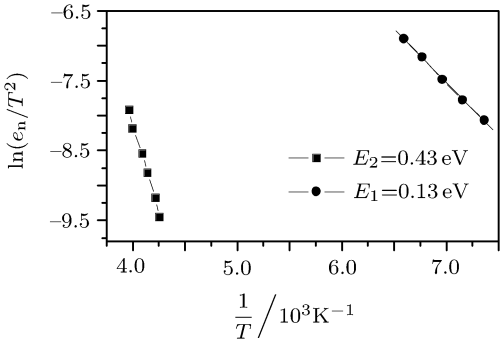


Fig.3. Arrhenius plots of deep levels for the sample 1202a.

3.3. $I-T$ characteristics

The $I-T$ behaviour of sample 1202a is shown in Fig.4(a). It is clear that the current rises with the temperature in an exponential manner. Since the voltage applied on the samples is constant, the curve mainly results from the thermo-emission mechanism, which depends on the temperature in the form of $I = A^*\exp(-\Delta E_b/kT)$, where ΔE_b is the active energy of the donor, and A^* is a constant. When the temperature increases, some of the electrons in the deep level are excited, as a result the charge carriers will "jump" from this level to the conduction band, and the current will increase, resulting in the peak shown in Fig.4(a). From the curve $\ln(I) - 1/T$ (Fig.4(b)), there are two obvious regions in the temperature range, which are nearly straight lines with different slopes. The temperature T=164.4 K can be considered as the turning point. A level (E_b) with an active energy of 0.13±0.01 eV can be obtained when the temperature is higher than 164.4 K. It is in good agreement with the position of E_1 detected by DLTS. Therefore, it can be considered that the energy level (E_c–0.13 eV) is caused by a defect with a temperature-activated capture cross section.[18]

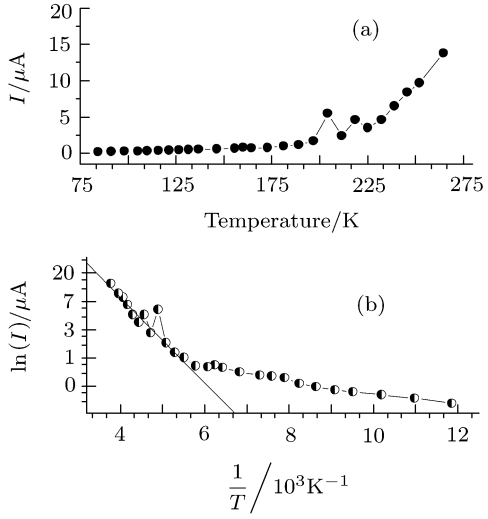


Fig.4. The temperature dependence of current of the sample 1202a. (a) curves of the experimental data. (b) $\ln(I)$ versus inverse temperature.

3.4. PL spectra

The room temperature PL spectra (line *a*) and Gaussian fit curves (lines *b* and *c*) for samples 1201p, 1202p and 1202a are shown in Fig.5, with the asymmetric PL line (dotted line). Two emissions (line *b* and line *c*) can be found by Gaussian fit. The positions of lines *b* and *c* and the intensities of the three samples are summarized in Table 1. The emission lines *b* are at 3.24, 3.25 and 3.27 eV for the samples 1202p, 1202a and1201p respectively. The emission lines *c* for these three samples are at 3.29, 3.29 and 3.30 eV, respectively. In order to know the origins of these emission lines, temperature dependence PL was measured (not shown here). When the temperature was decreased from room temperature to 83 K, the intensity of the dominant emission at 3.30 eV increased rapidly and the value of full-width at half–maximum

(FWHM) was decreased. In addition, the peak position shifted to high energy side when the temperature decreased. All these characters indicated that this emission (line c) could be attributed to the free exciton (FE) recombination.[19] Compared with emission line c, emission line b has a lower emission energy and wider FWHM. Considering about the defect state emission in semiconductor, the energy position of the luminescence line b can be given by Eq.(4)[20]

$$E_{\text{emission}} = E_{\text{g}} - E_{\text{d}} + kT/2, \tag{5}$$

where E_{emission} is the emission energy; E_{g} is the optical energy gap and E_{d} is the ionization energy of the defect. In Table 1, the parameter E_{d} was calculated at room temperature, as defined by Eq.(4). Under experimental error control, the calculated defect-related luminous centre is quite close to that detected by DLTS and $I-T$. In addition, it can be found that the intensity of emission line b is affected by the relative defects concentration of level E_1. Therefore, we speculate that the level E_1 is a localization state deep level, and has a close relationship with luminescence centres. The electrons on level E_1 have transferred to valence band and result in the electron-cavity combined luminescence (D^0h). While, with increasing flux of eluting gas, the position of E_1 level has a little shift to the conduction band. The relationship between the position of E_1 and the sample growth eluting gas condition indicates that E_1 has a characteristic of microstructure defect. Baltrameyunas[21] investigated the effect of photo-induced absorption in wide-gap II–VI semiconductors with heat treatment effect on the stoichiometry and the concentration of point defects. The interstitial Zni defect is relatively a shallow donor (0.1–0.2 eV) in zinc chalcogenides. Local disturbances of interstitial centres will result in mutual renormalization of the band and shallow-defect states at much lower concentrations than chemical substitutional impurities. Therefore, we suspect that the shift of location of E_1 and the increment of relative trap density are induced by the interstitial Zni concentrations.

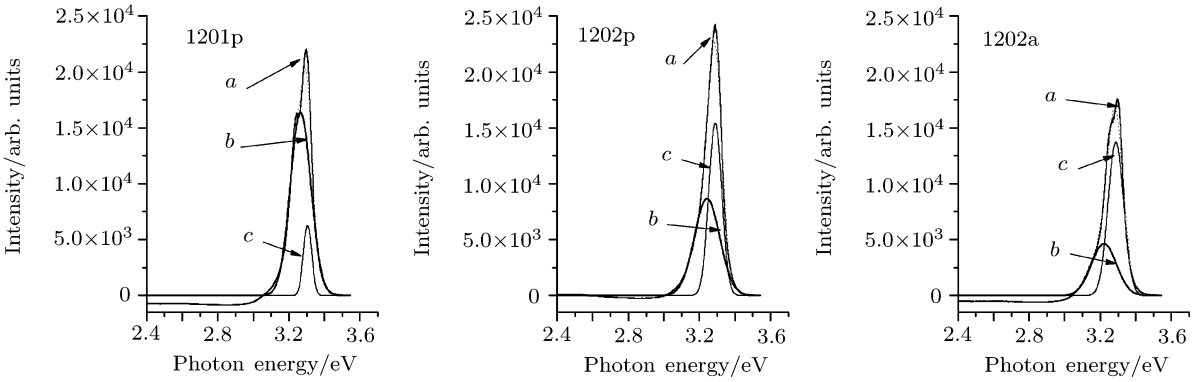


Fig.5. The PL spectra of samples 1201p, 1202p, 1202a at room temperature for different carrier gas rates; a is experiment curve, b and c are Gauss fit curves.

Table 1. The characteristics of deep levels and photoluminescence for samples prepared in N_2.

(Sample) number	(N_2 flux) (slm)	DLTS measurement E_{T} /eV	DLTS measurement ($N_{\text{t}}/N_{\text{B}}$) /%	PL spectrum fit parameter (line b) E_{emission}/eV	PL spectrum fit parameter (line c) E_{emission}/eV	PL spectrum fit parameter (intensity) /arb. units	E_{d} /eV
1202p	0.86	E_1=0.15±0.06	1.34	3.24		8700	0.140
					3.29	16419	
		E_2=0.47±0.07	3.39				
1202a	1.4	E_1=0.13±0.02	1.01	3.25		4620	0.133
					3.29	14274	
		E_2=0.43±0.05	5.10				
1201p	1.7	E_1=0.09±0.04	1.99	3.27		16682	0.113
					3.30	6450	
		E_2=0.41±0.07	8.71				

Note: ($N_{\text{t}}/N_{\text{B}}$) is relative trap density; (E_{d}) is Ionization energy; (E_{emission}) is light emitting energy.

As to the deep energy centre E_2 which was detected by DLTS, it is seen that this kind of the defect has a larger relative trap density, and the level position shifts to the conduction band under higher eluting gas. Unfortunately, the emission related to level E_2 is not found during the PL measurement. However, E_2 has an influence on excitation emission. When the relative trap density of E_2 increases, the emission intensity of FX decreases (see Table 1). The origin of deep level E_2 will need further research, as there are many defects and complicated defect structure in ZnO.

4. Conclusion

In this work, ZnO/Si heterostructure were deposited by MOCVD and two deep levels of E_1 (E_C–0.13±0.02 eV) and E_2 (E_C–0.43±0.05 eV) were found. In addition, the defect level E_1 related emission was detected in the PL spectra and the origination of E_1 was considered to be the interstitial Zni in ZnO. Deep level E_2 is act as a recombination centre, while it also has an influence on the free exciton emission intensity.

Acknowledgments

The authors would like to acknowledge Junjie Zhu from Physics Department of University of Science and Technology of China, for his powerful support in the sample fabrication and PL spectrum measurement.

References

[1] Van de Pol F C M, Blom F R and Popma T J A 1991 *Thin Solid Films* **204** 349
[2] Gorla C R, Emanetoglu N W, Liang S, Mayo W E, Lu Y, Wraback M and Shen H 1999 *J. Appl. Phys.* **85** 2595
[3] Gao P X and Wang Z 2005 *J. Appl. Phys.* **97** 044304
[4] Sun H, Zhang Q F and Wu J L 2007 *Acta Phys. Sin.* **56** 3479 (in Chinese)
[5] Yang G and Santos Paulo V 2007 *Acta Phys. Sin.* **56** 515 (in Chinese)
[6] Vayssieres L, Keis K, Hagfeldt A and Lindquist S E 2001 *Chemistry of Materials* **13** 4395
[7] Chu T L and Chu S S 1995 *Solid-State Electronics* **38** 533
[8] Keis K, Magnusson E, Lindström H, Lindquist S-E and Hagfeldt A 2002 *Solar Energy Materials and Solar Cells* **73** 51
[9] Li H X, Liu H, Wang J Y, Yao S S and Cheng X F 2004 *Mater. Lett.* **58** 3630
[10] Zhu J J, Lina B X, Sun X K, Yao R, Shi C S and Fu Z X 2005 *Thin Solid Films* **478** 218
[11] Liu C H, Chen Y L, Zhu J J, Fu Z X, Lin B X, Peng C and Yang Z 2001 *Chin. Phys. Lett.* **18** 1108
[12] Sze S M 1981 *Physics of Semiconductor Devices* (New York: Wiley) 255
[13] Nikitin S E, Nikolaev Yu A, Polushina I K, Rud V Y and Terukov E I 2003 *Semiconductors* **37** 1291
[14] Cevdet Coskun, Nebi Gedik and Ercan Balc 2006 *Semicond. Sci. Technol* **21** 1656
[15] Simpson J C and Cordaro J F 1988 *J. Appl. Phys.* **63** 1781
[16] Tang X, Clauzonnier A, Campbell H I, Prior K A and Cavenett B C 2004 *Appl. Phys. Lett.* **84** 3043
[17] Lang D V 1974 *J. Appl. Phys.* **45** 3023
[18] Auret F D, Goodman S A, Legodi M J, Meyer W E and Look D C 2002 *Appl. Phys. Lett.* **80** 1340
[19] Zhu J J, Yao R, Liu C H, Lee In-Hwan, Zhu Lala, Ju Jin-Woo, Back Jong Hyebob, Lin B X and Fu Z X 2006 *Thin Solid Films* **514** 306
[20] Tamura K, Makino T, Tsukazaki A, Sumiya M, Fuke S, Furumochi T, Lippmaa M, Chia C H, Segawa Y, Koinuma H and Kawasaki M 2003 *Solid State Communications* **127** 265
[21] Baltrameyunas R, Gavryushin V, Rachyukatiis G, Kazlauskas A, Ryzhikov V D, Markov E V, Teplitskii V A, Kamenskii M A and Smirnov 1991 *Sov. Phys. Solid State* **33** 537